Review of AWE multi-material radiation-hydrodynamics capabilities

R. P. Smedley-Stevenson
CPG/DPD AWE

Multi-material meeting, Prague, 10-14/09/2007

Some Acknowledgements

- Taylor et al. *Jet examples*
- Stevenson et al. *NIF hohlraum*
- Hughes *ICF capsule calcs.*
- Taylor *Fill tube examples*

Contents

- Brief overview of AWE codes
- Present results for AGEX-II applications
  - Counter propagating jets
  - NIF hohlraum
  - ICF capsule modelling
    - Discuss the impact of the ray effect
  - ICF fill tube modelling – planar geometry

AWE rad-hydro codes

- Legacy
  - NYM
    - 1D/2D Lagrangian
    - 3T grey+MG diffusion/IMC
    - Laser energy deposition/NLTE
  - PETRA
    - 2D Eulerian
    - 3T grey+MG diffusion
- Modern
  - CORVUS
    - 2D ALE
    - 2T grey+MG diffusion/Sn/IMC
    - Laser energy deposition/NLTE
  - SHAMROCK
    - 2D Eulerian/AMR
    - 1T grey diffusion
  - PEGASUS
    - 3D ALE
    - 2T grey+MG diffusion
  - HYDRA
    - 3D Eulerian/(AMR soon)
    - 1T grey diffusion

Multi-physics solution strategy

- Operator splitting
  - Staggered grid hydro algorithm - Lagrange+re-map
    - Uses P_{rad} and dE/dt(rad)
  - Radiation transport solved at end of the advection step using new mesh
    - Deposits dE/dt(rad) for hydro sub-cycling
  - Similar strategy for other physics

AGEX-II applications

- Jet interaction experiments (OMEGA laser at Rochester)
  - Single jet calibration
  - Colliding jets/counter propagating shocks
  - Crude hohlraum modelling for late time pressure effects
- CORVUS models of NIF hohlraum
  - Recent test of new laser physics options
- Investigation of the ray effect
  - Non-uniformity of hohlraum illumination
  - Symmetric ICF capsule implosions
- ICF fill tube modelling – planar geometry (LLNL collaboration)

Single Jet

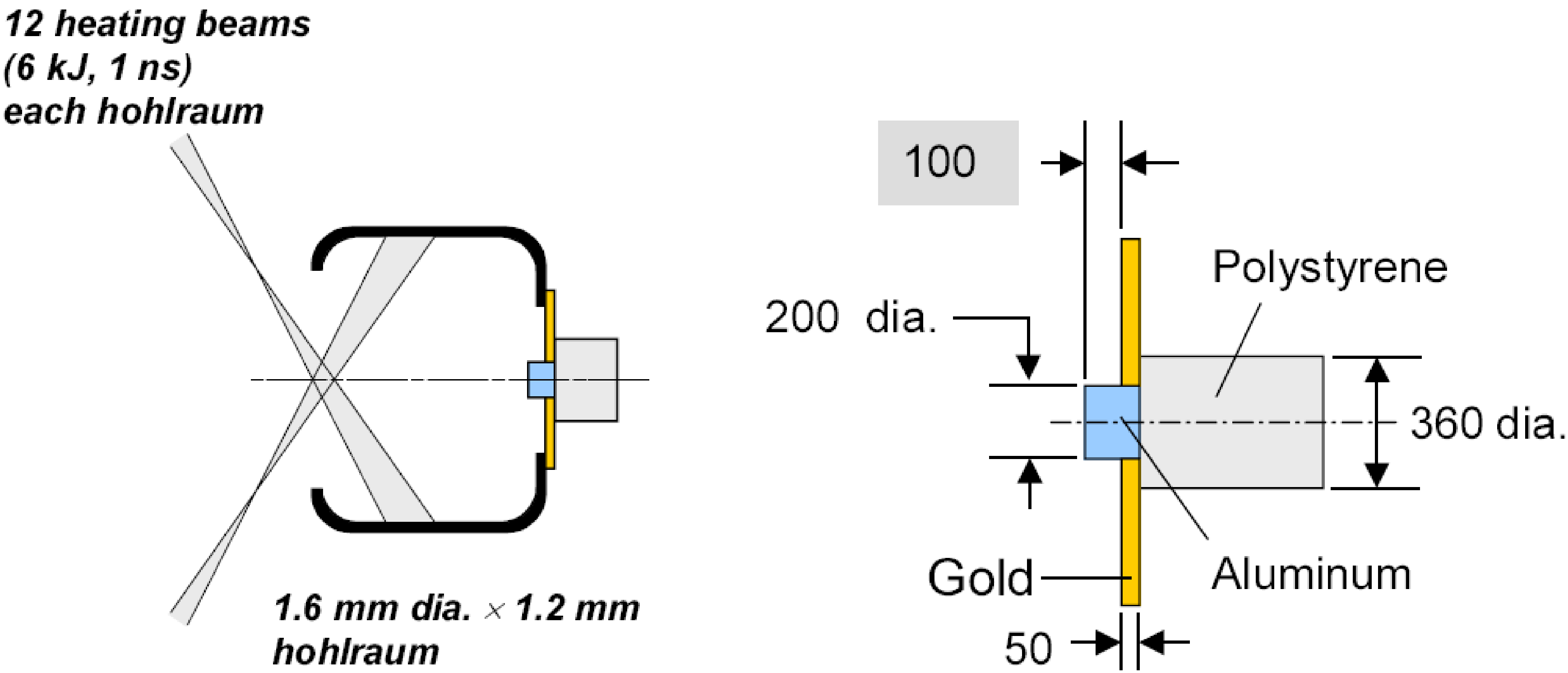

Figure 1: Test case for an indirectly-driven jet experiment. The hohlraum and experimental package (left) and the dimensions (μm) of the target (right).

Calibration of the hydrodynamics

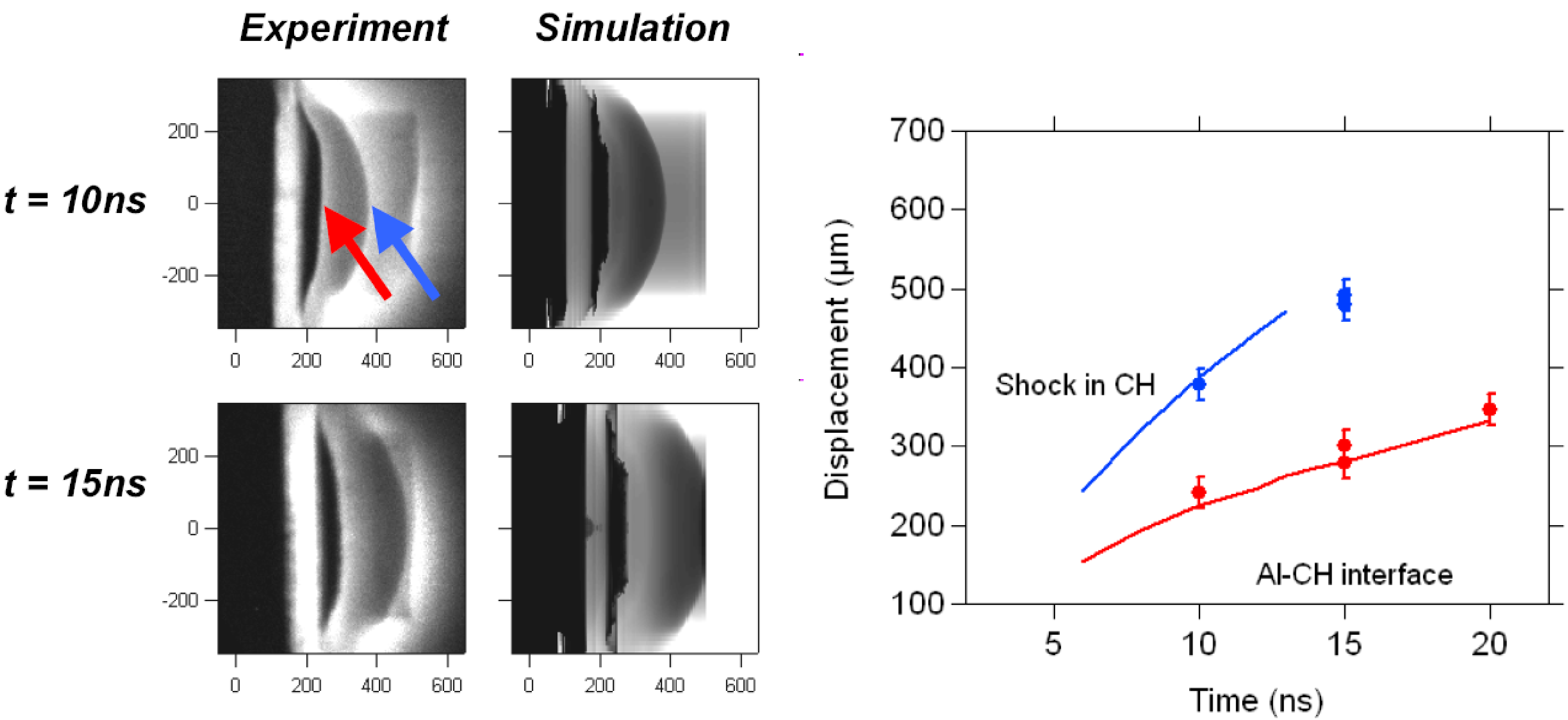

Figure 4(a) Simulated and experimental radiographs of a planar shock target, identifying the location of the bowshock and Al-CH interface. (b) Displacement-time plot demonstrating that the reference calculations are a good match to the experimental data.

CORVUS simulations

- ALE mesh vs Eulerian mesh
  - ALE allows greater resolution at the shock fronts
  - Density is shown superimposed on the mesh

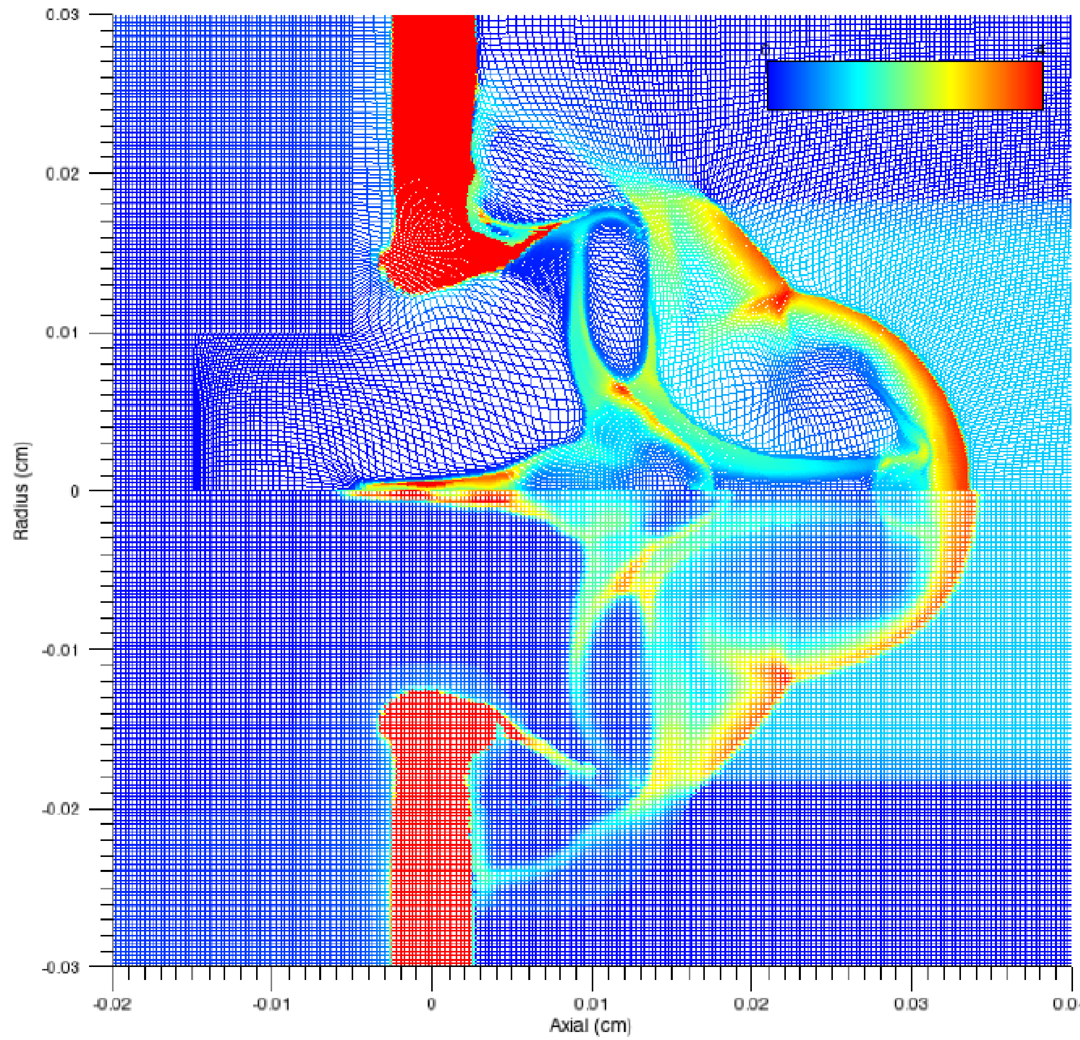

SHAMROCK results

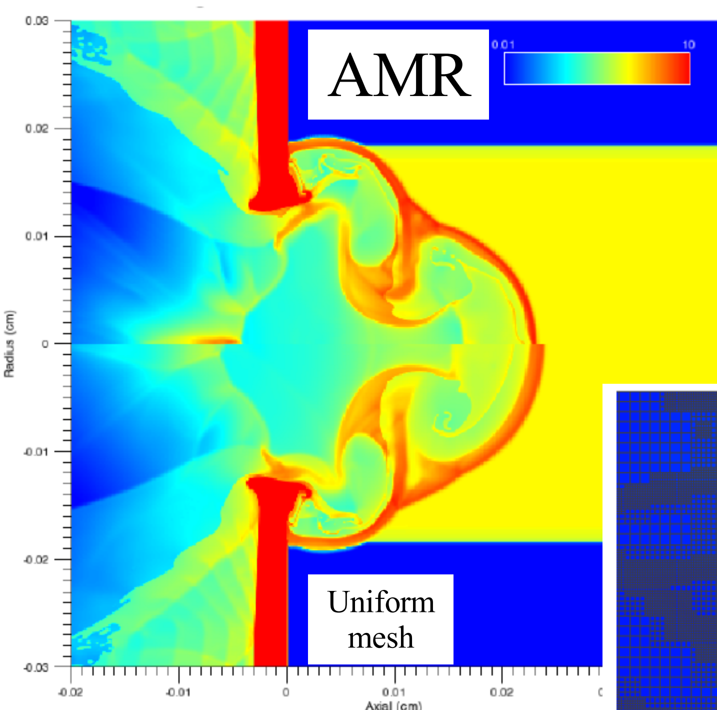

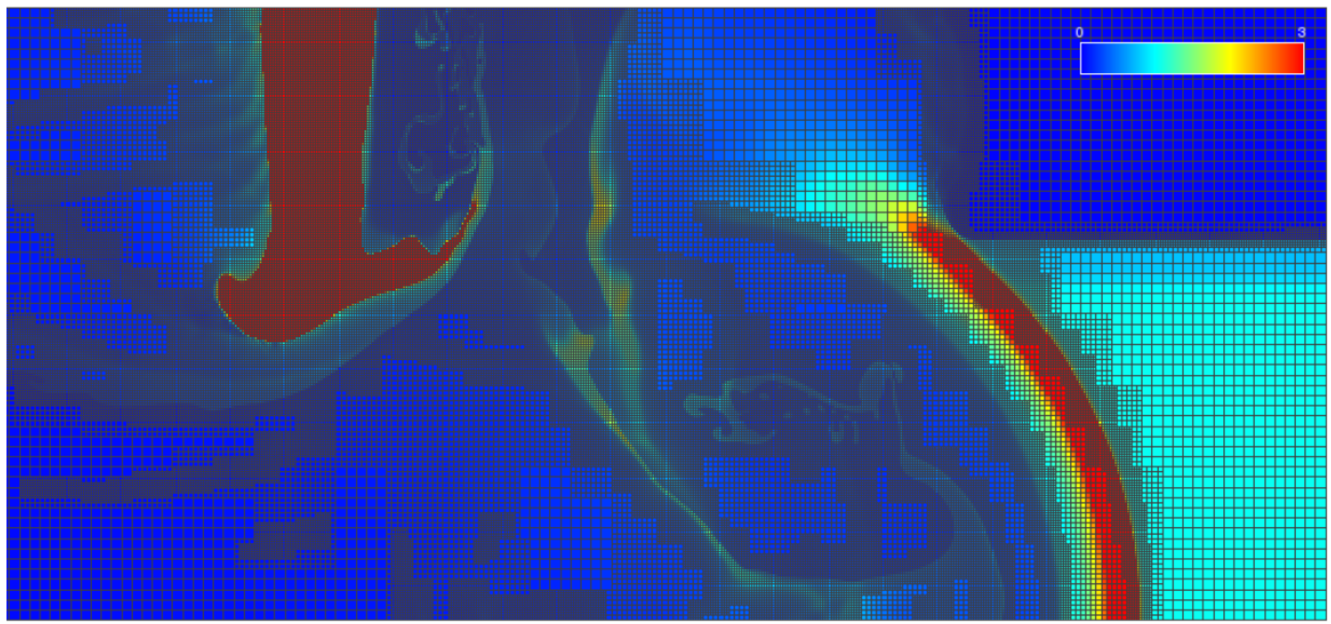

Figure 16: AMR calculation of a supersonic jet at 9ns. Use of tuned mesh refinement criteria allows regions of interest to be highly resolved and substantially reduce the total number of cells required.

Counter-propagating Jets

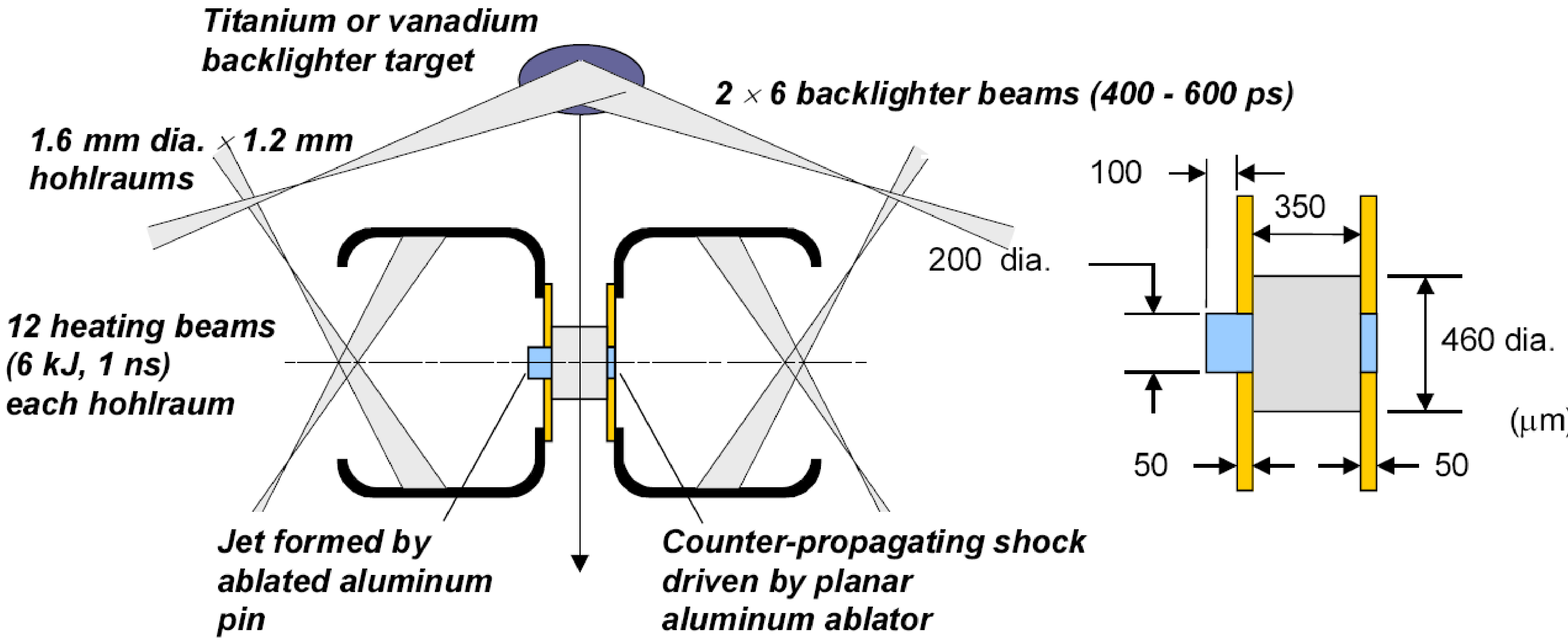

Figure 2: Test case 3 for indirectly-driven jet experiment. This is the jet-shock interaction target, designed to test the interaction of a jet with a planar shock. Figure 2a (left) shows the whole target assembly and Figure 2b shows the dimensions of the experimental package.

CORVUS results

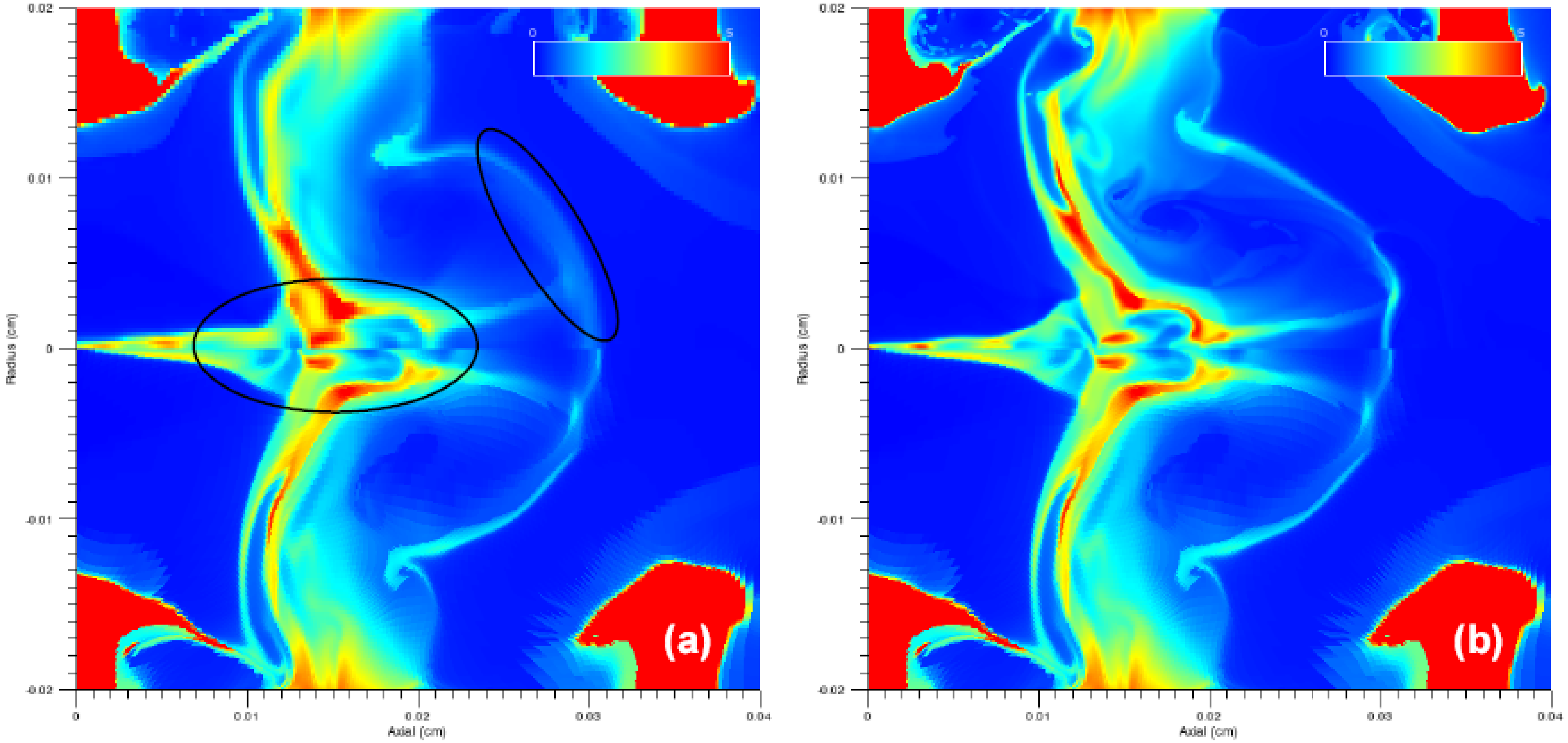

Figure 22: These are simulations of the counter-propagating jet-shock experiment at 8.8ns. Figure 22(a) compares a 2.5µm Eulerian calculation (top) with a 2.5µm ALE calculation, with the most significant differences highlighted. Figure 22(b) shows 1.25µm Eulerian and 2.5µm ALE results.

2D-3D Eulerian comparison

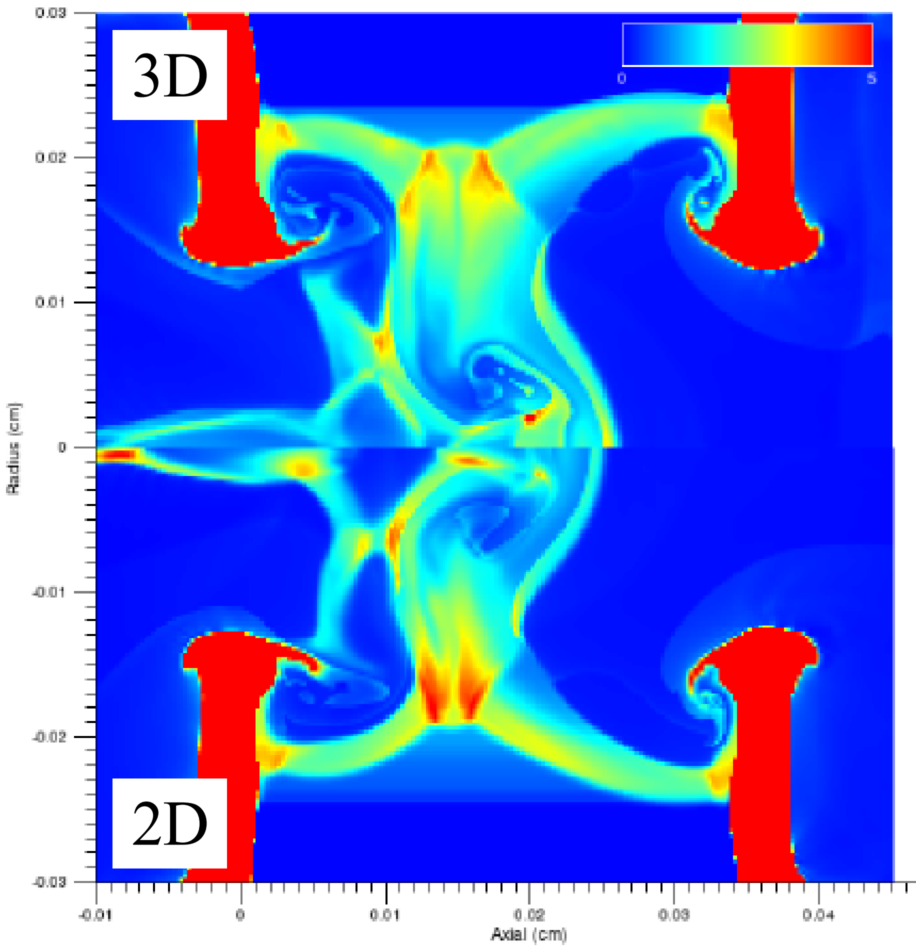

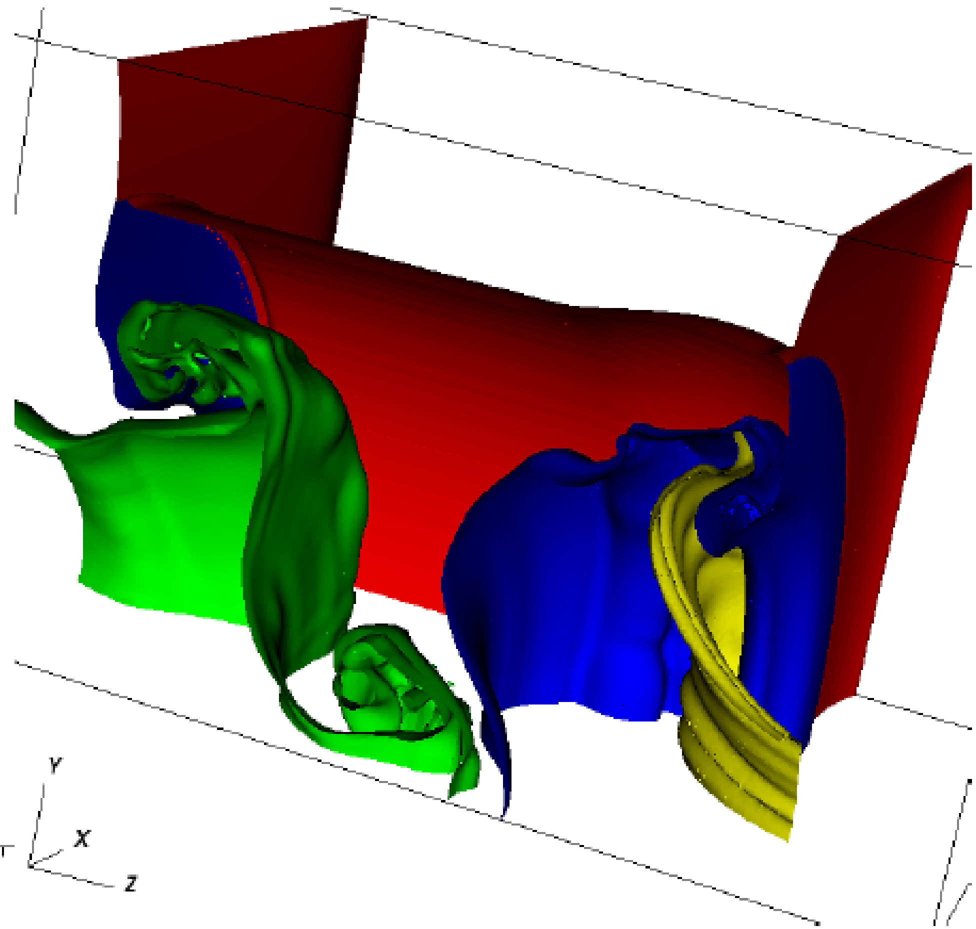

Early attempts at hohlraum modelling

- Laser modelled as a uniform energy source in the hohlraum volume
  - Attempt to better model late time pressure drive from the hohlraum

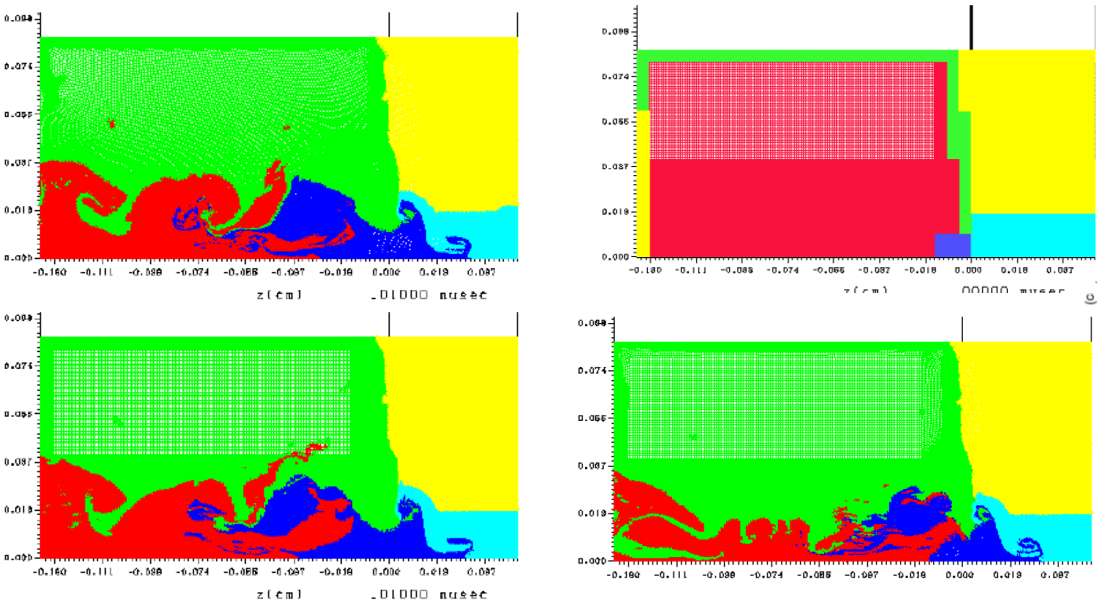

CORVUS

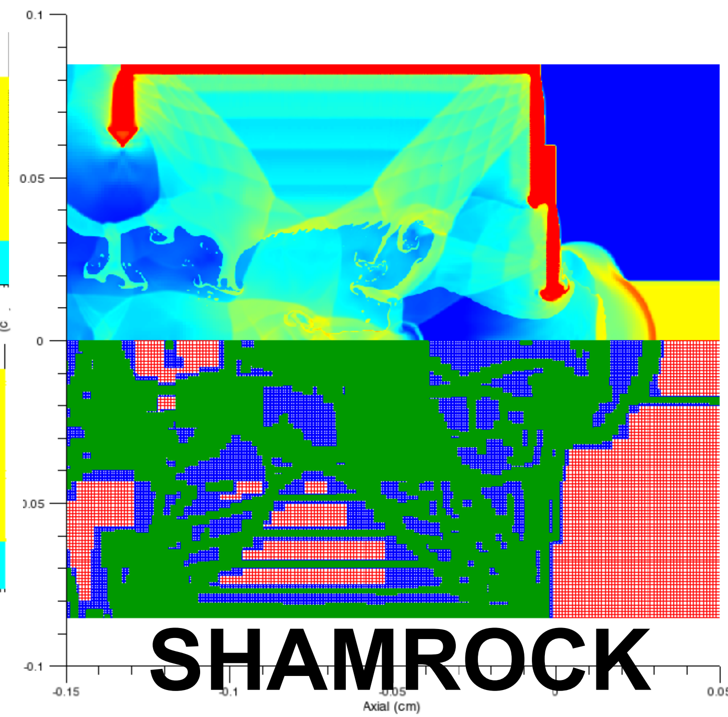

SHAMROCK

Figure 18: An AMR integrated hohlraum calculation at 7ns. Density (log-scale) is compared with the calculational mesh (bottom); colours indicate the refinement level.

CORVUS simulations of a NIF hohlraum design

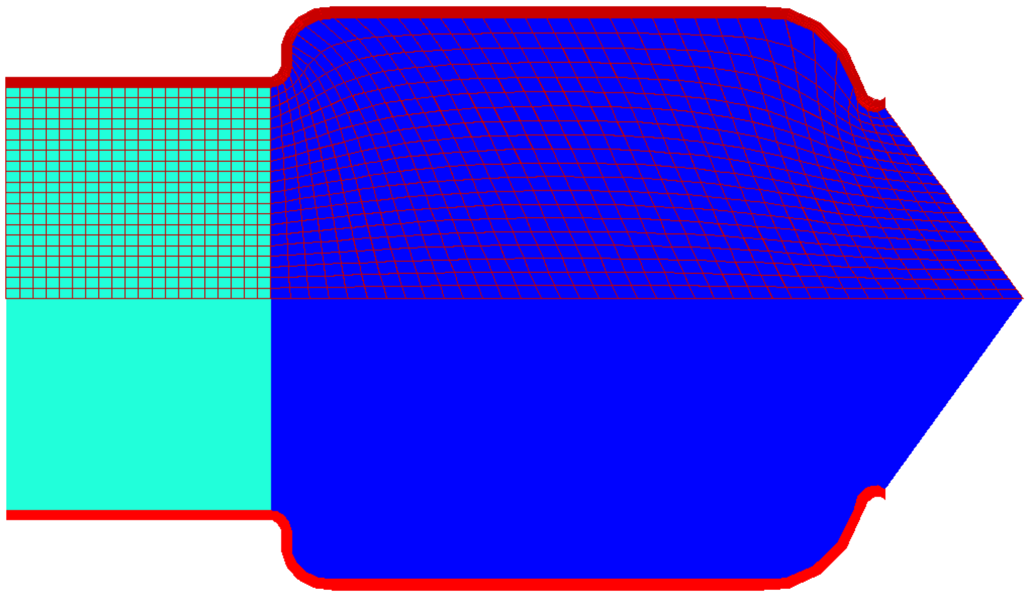

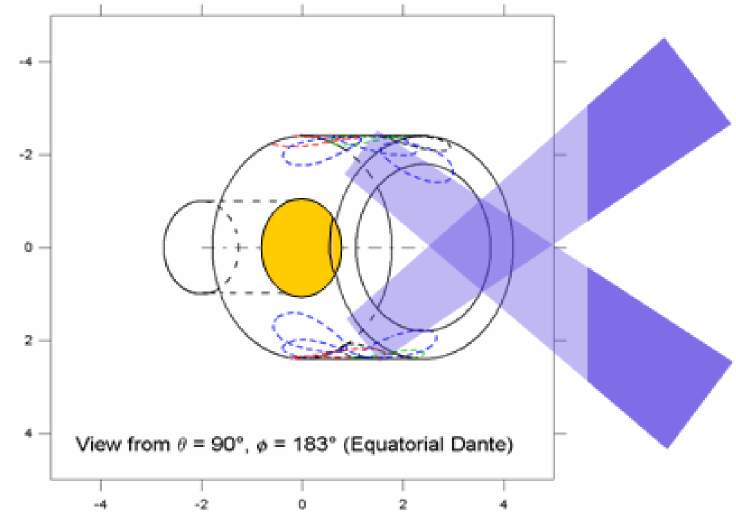

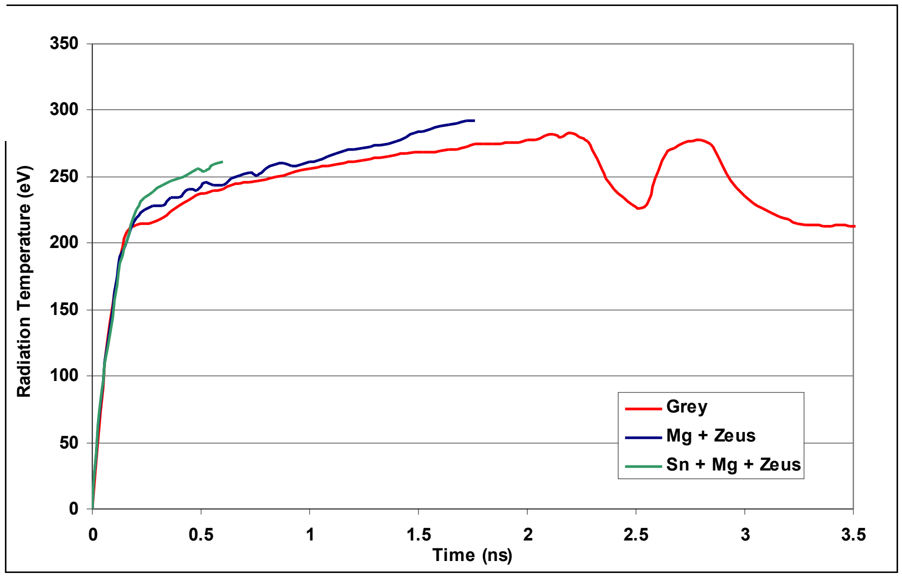

CORVUS laser energy deposition results

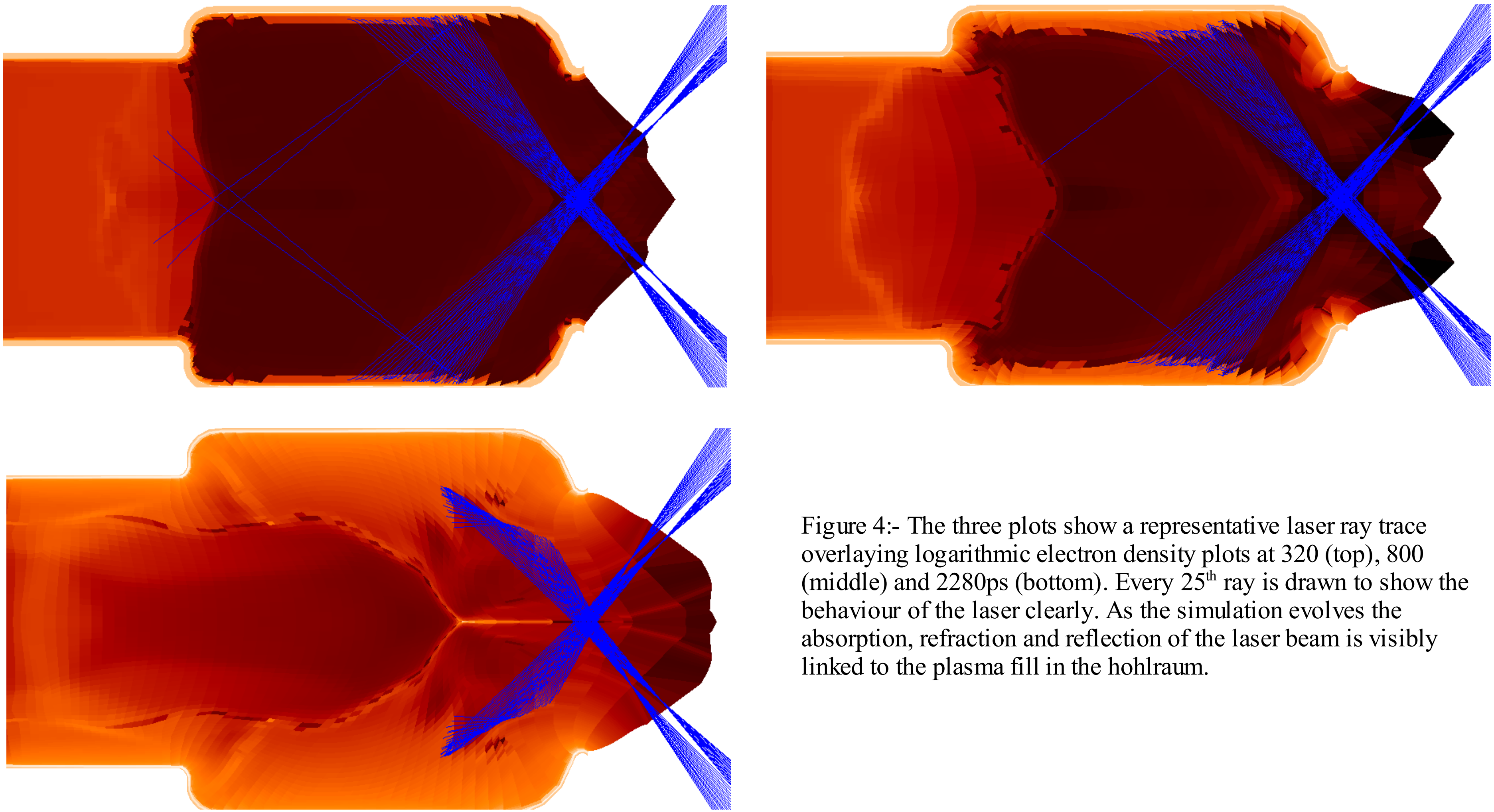

Figure 4:- The three plots show a representative laser ray trace overlaying logarithmic electron density plots at 320 (top), 800 (middle) and 2280ps (bottom). Every 25th ray is drawn to show the behaviour of the laser clearly. As the simulation evolves the absorption, refraction and reflection of the laser beam is visibly linked to the plasma fill in the hohlraum.

CORVUS hohlraum calcs.

- Calculations would not have been possible without:
  - Addition of new physics models
    - Laser ray-trace
    - Non-LTE
  - Improvements to ALE mesh movement
  - Compatible hydro algorithm

Ray effects/Angular convergence

- Sn transport calculations are prone to the ray effect
  - Particles can only travel along the quadrature directions
    - Attenuation calculated correctly but beams have infinitesimal width – unable to model $1/r^2$ fall-off correctly
    - Leads to artificially high fluxes along the ray directions, with a flux deficit in-between
- Assess the severity of the ray effect for ICF capsule implosions
  - Example of fill tube modelling

Hohlraum test problem

- High Sn order required to resolve the angular dependence of the flux on the capsule

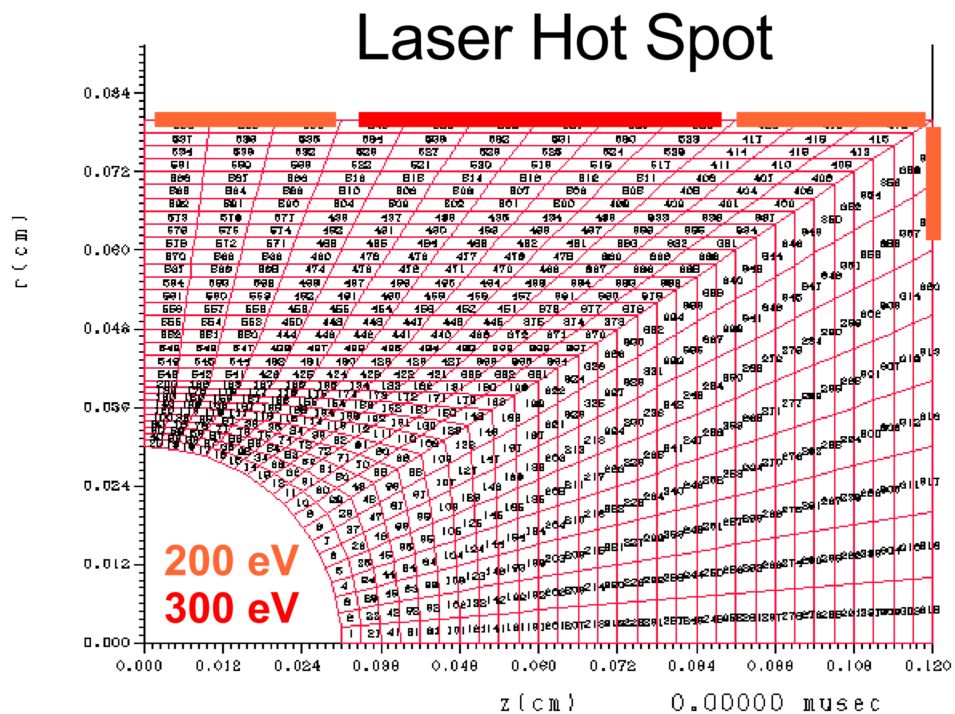

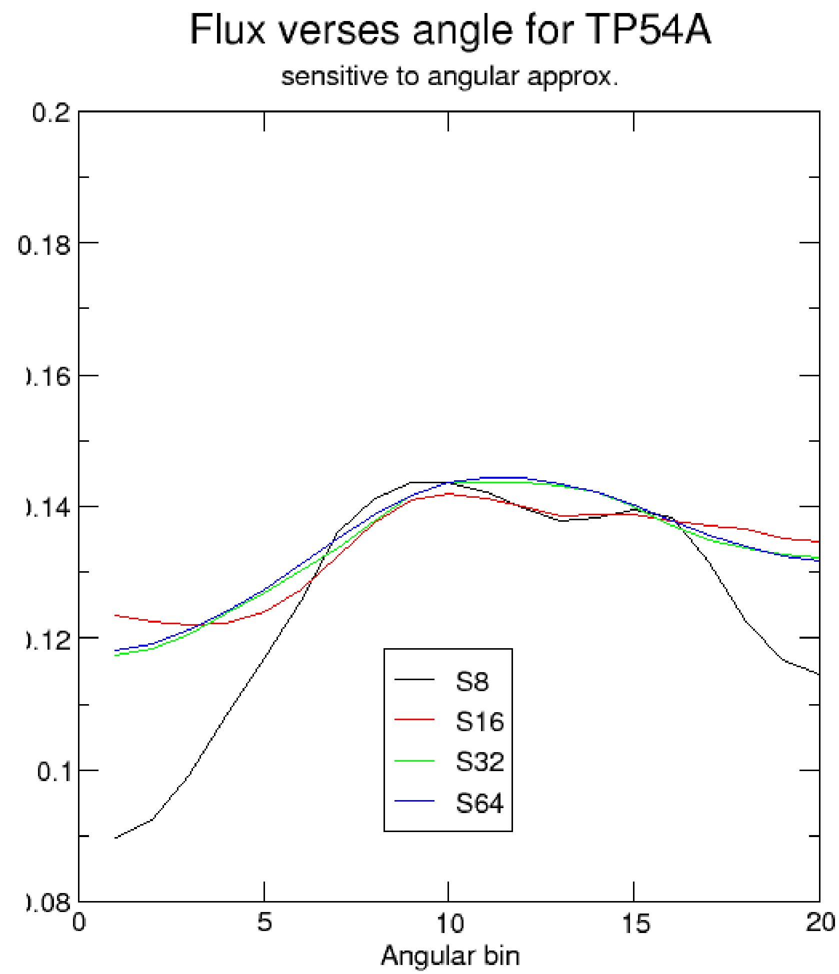

ICF capsule implosion – S4 verses S8

4.5 ns

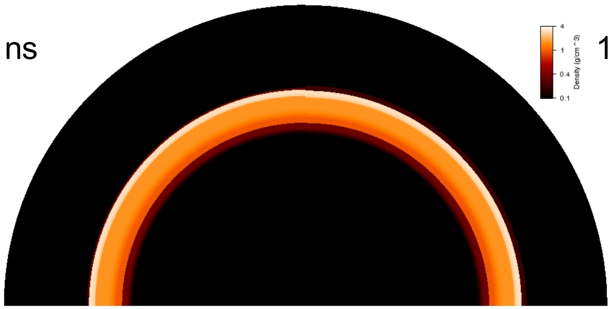

10.5 ns

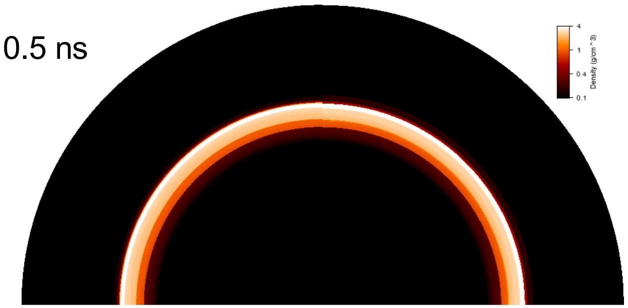

15 ns

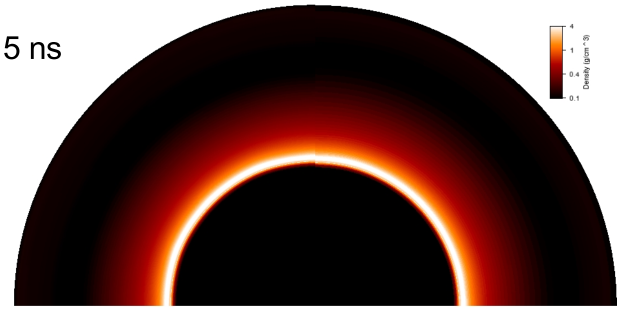

15.5 ns

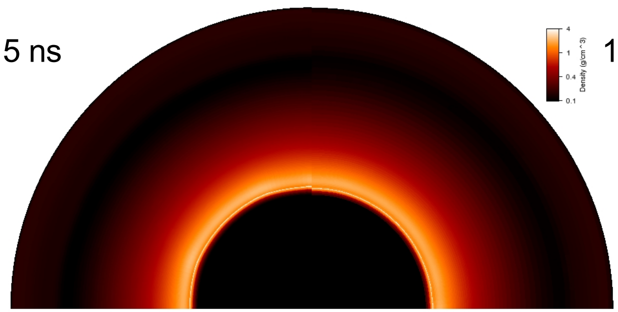

16 ns

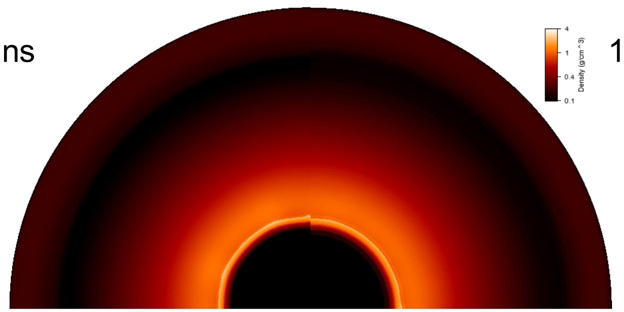

16.2 ns

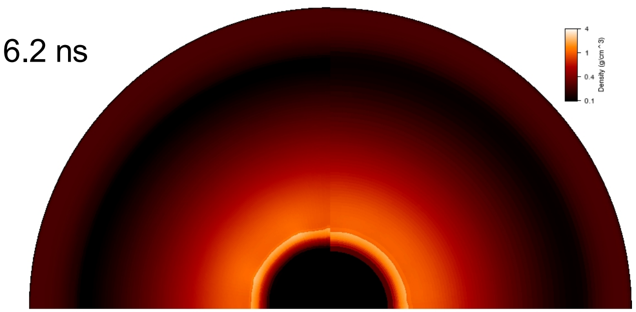

16.4 ns

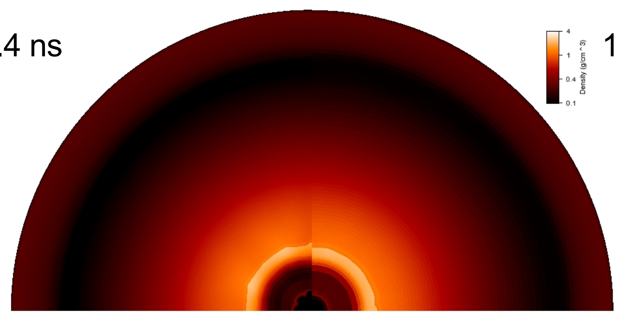

16.6 ns

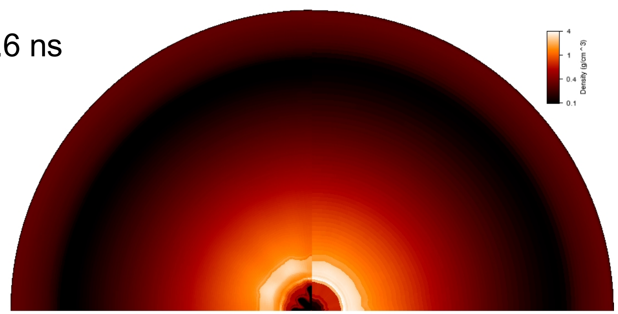

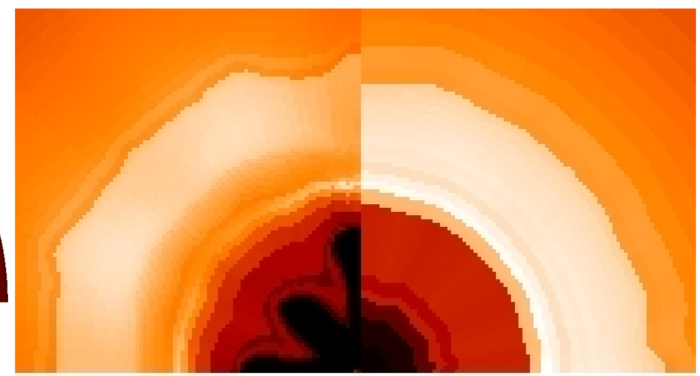

ICF capsule implosion – S4 verses S8

S4 @ 16.6 ns

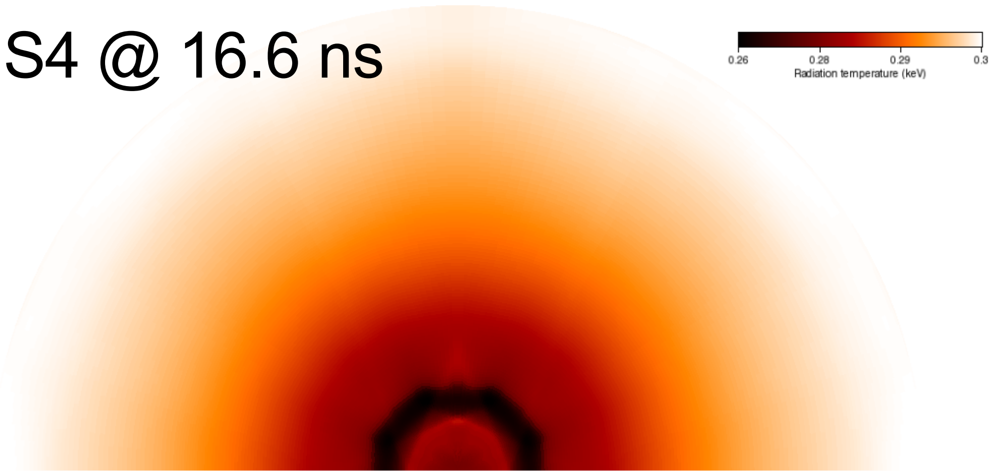

S8 @ 16.6 ns

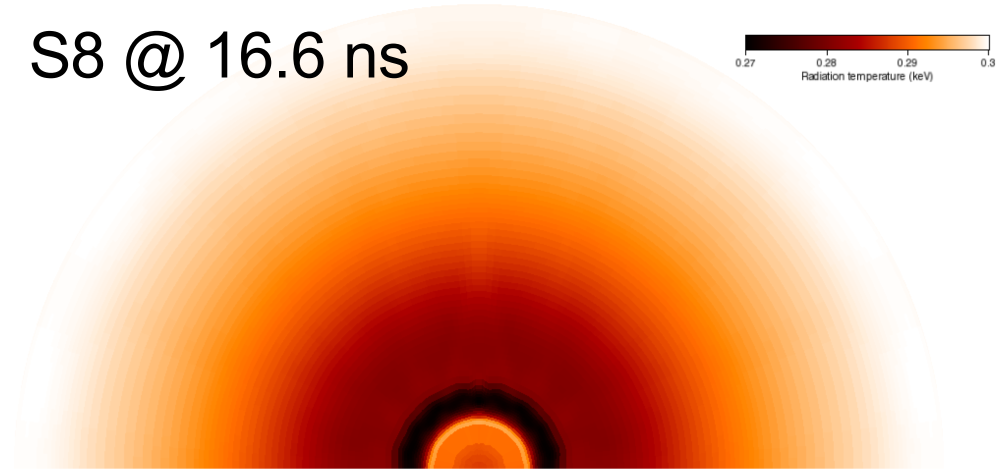

S8 @ 16.7 ns

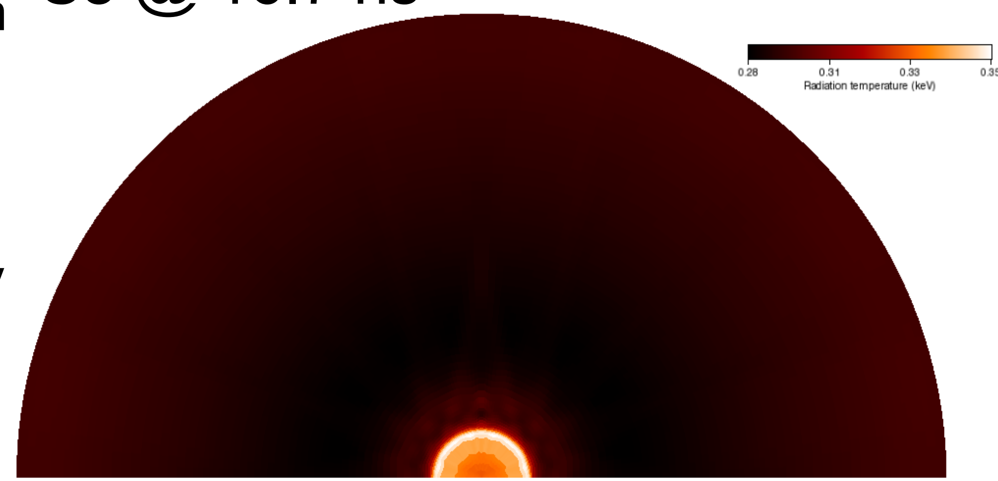

- Ray effects are apparent in the radiation field in the centre of the capsule
  - Symmetry of the implosion is compromised
- High Sn is order essential in both the hohlraum and the capsule, to accurately model the implosion symmetry

ICF capsule fill tube modelling

A narrow glass tube inserted ~ few x 10µm into the ablator delivers DT through a hole ~ few µms diameter

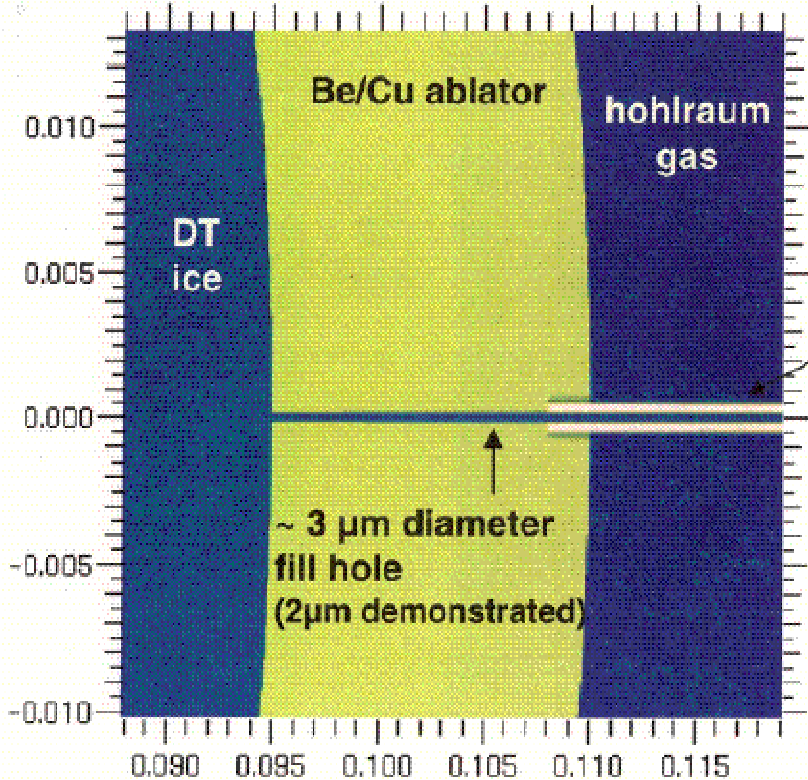

The design objective is to minimize the perturbation of realistic options on the implosion

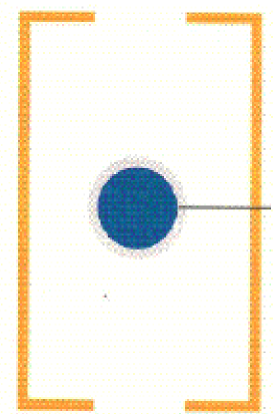

Hohlraum with the ICF capsule suspended in the centre. The fill tube is connected to a reservoir of DT

Planar variant of ICF fill tube

Planar version to study the jet growth and evolution. The entire mesh is illustrated below. This subtends an angle of ~2.6 degrees. The entire mesh has ~26k cells. 7 cells across the inner 6um diameter of the tube, with 5 zones in the wall of the tube. Pure **EULERIAN** mesh movement.

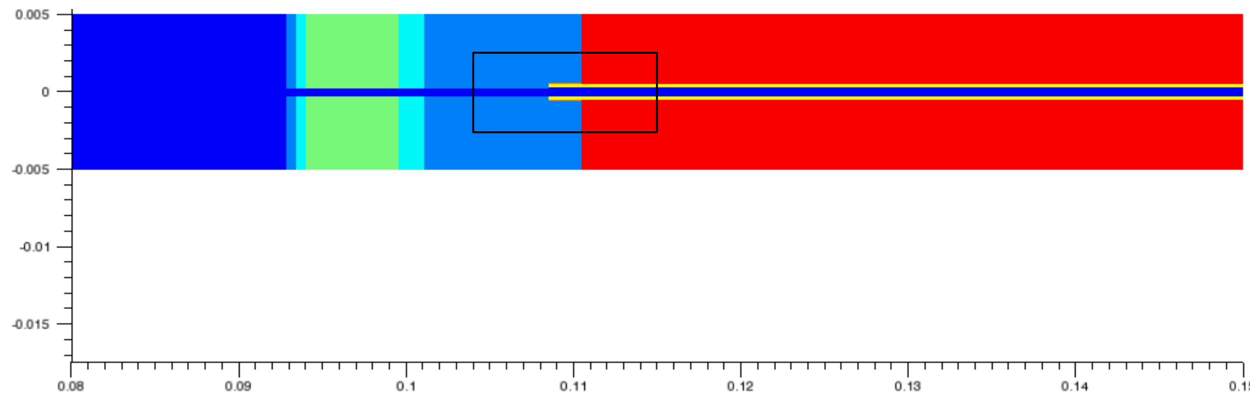

4 Phases of the Implosion:

1) Shock transit - initial tube explosion, jet formation & establishment of “preferred mode”
2) Implosion & RT growth phase
3) Stagnation & RT growth phase
4) Ignition & burn

Modelling such a small region limits us to studying only the first phase of the implosion.

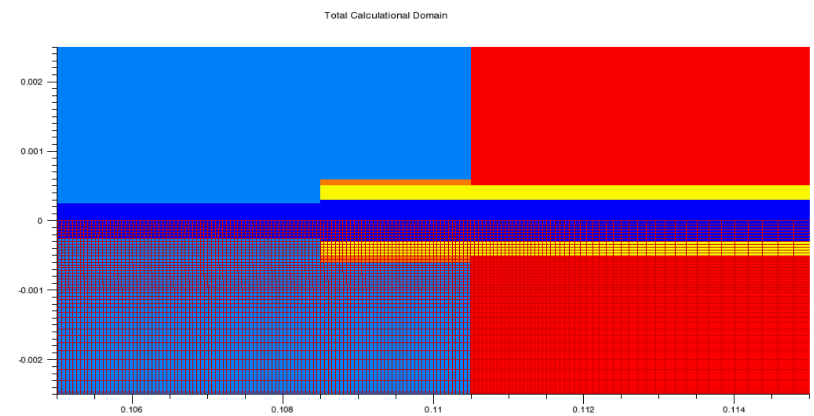

ICF fill tube results

Comparing diffusion (top) with S8 transport.

Both runs with Planckian temp drive applied at fixed boundary. Eulerian hydro. Clearly drive in diffusion case needs to be scaled to match transport solution.

Worryingly the seed for future RT growth looks larger in the transport case than in the diffusion case.

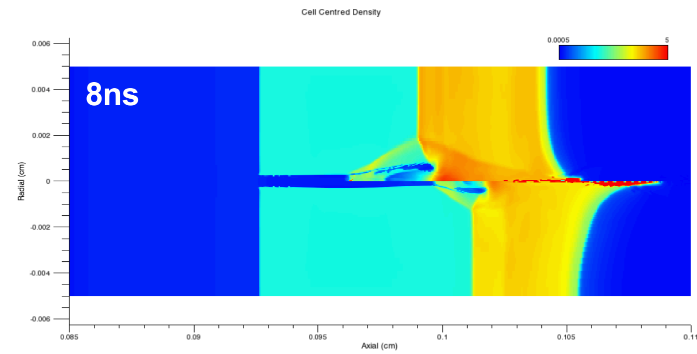

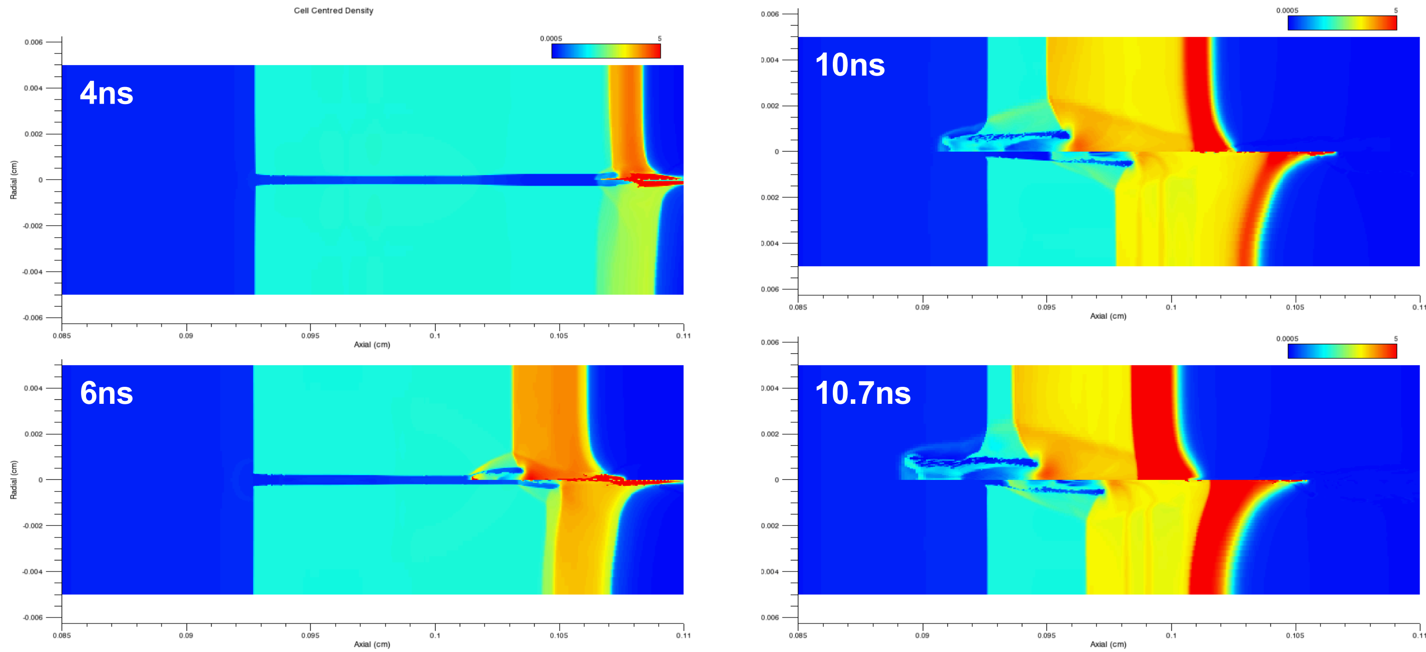

Transport produces different results

- Jet penetrates less far into the capsule - reduced radiation flow through the tube
- The transverse shocks in the ablator are significantly weaker
- Seed for subsequent low-mode RT growth is larger, which could potentially degrade the yield.

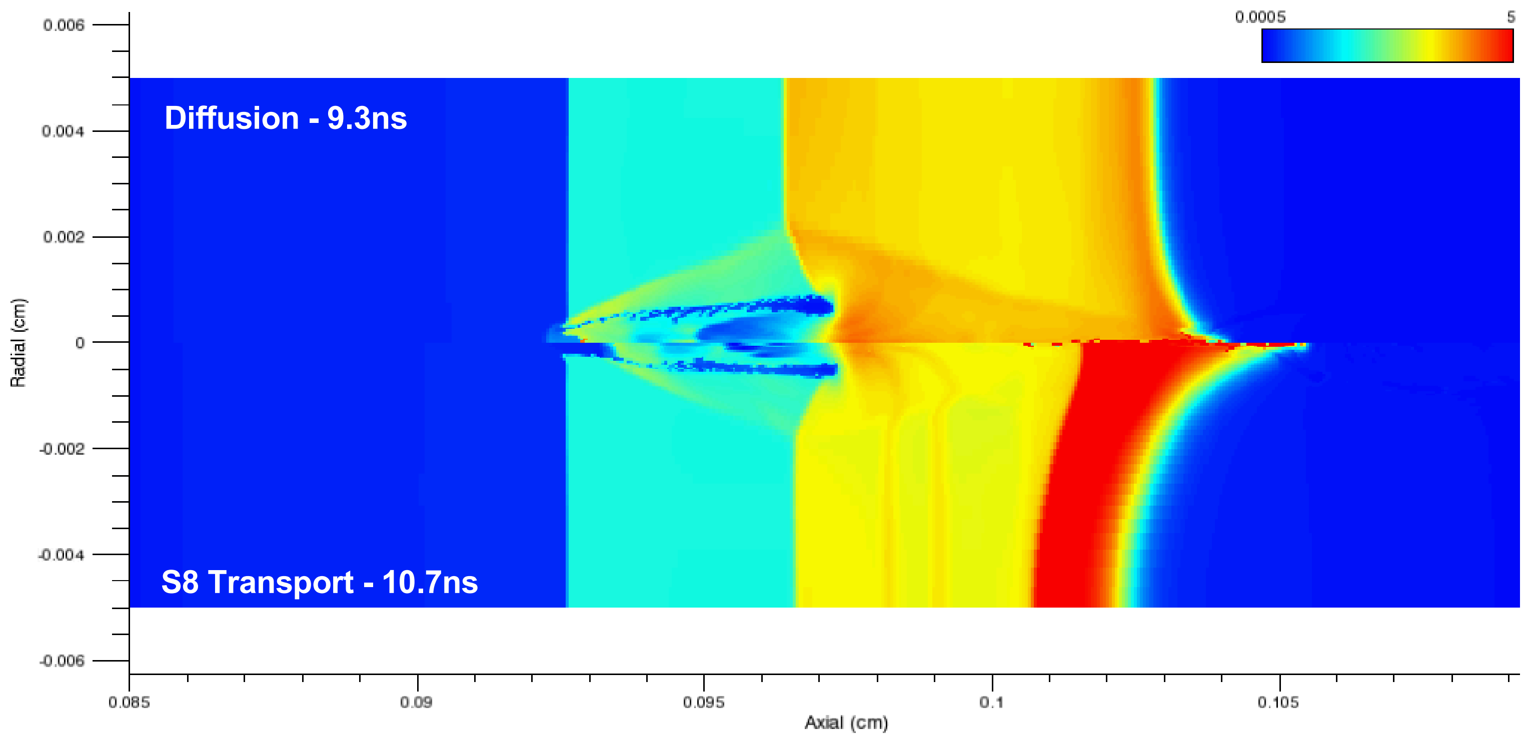

Conclusions

- Presented an overview of AWE capabilities
- Illustrated need for high Sn orders/MC to model capsule implosions
  - Significant challenge to develop high fidelity models – scalable parallelism is essential